

Infrared behavior of gluon and ghost propagators from asymmetric lattices

Attilio Cucchieri¹ and Tereza Mendes¹

¹*Instituto de Física de São Carlos, Universidade de São Paulo,
C.P. 369, 13560-970, São Carlos, SP, Brazil*

We present a numerical study of the lattice Landau gluon and ghost propagators in three-dimensional pure $SU(2)$ gauge theory. Data have been obtained using asymmetric lattices ($V = 20^2 \times 60, 40^2 \times 60, 8^2 \times 64, 8^2 \times 140, 12^2 \times 140$ and $16^2 \times 140$) for the lattice coupling $\beta = 3.4$, in the scaling region. We find that the gluon (respectively ghost) propagator is suppressed (respec. enhanced) at small momenta in the limit of large lattice volume V . By comparing these results with data obtained using symmetric lattices ($V = 60^3$ and 140^3), we find that both propagators suffer from systematic effects in the infrared region ($p \lesssim 650\text{MeV}$). In particular, the gluon (respec. ghost) propagator is less IR-suppressed (respec. enhanced) than in the symmetric case. We discuss possible implications of the use of asymmetric lattices.

PACS numbers: 11.15.Ha, 12.38.Aw, 12.38.Lg, 14.70.Dj

I. INTRODUCTION

Gluon and ghost propagators are powerful tools in the (non-perturbative) investigation of the infra-red (IR) limit of QCD and are thus of central importance for understanding confinement (see for example [1, 2]). In fact, according to the Gribov-Zwanziger [3, 4, 5, 6, 7] and to the Kugo-Ojima [8, 9] confinement scenarios in Landau gauge, the ghost propagator must show a divergent behavior — stronger than p^{-2} — for vanishing momentum p . This strong infrared divergence corresponds to a long-range interaction in real space, which may be related to quark confinement. At the same time, according to the former scenario, the gluon propagator must be suppressed and may go to zero in the IR limit [3, 4, 5, 6, 7, 10, 11, 12]. This would imply that the real-space gluon propagator is positive and negative in equal measure, i.e. reflection positivity is maximally violated [13, 14], indicating absence of gluons from the physical spectrum (gluon confinement). These predictions are also valid for the case of pure $SU(2)$ gauge theory and for three space-time dimensions.

The nonperturbative evaluation of gluon and ghost propagators can be achieved by first principles methods such as Dyson-Schwinger equations (DSE's) [1, 2] or the numerical simulation of lattice QCD. In the latter case, special care must be taken to eliminate finite-size effects, especially in studies of the IR region [15, 16, 17, 18]. These two approaches have produced consistent results, confirming the predictions mentioned above for the divergence of the ghost propagator and for the suppression of the gluon propagator in the IR limit. More specifically, Landau-gauge studies of DSE's (see for example [19, 20, 21]) have found an IR behavior of the form $D(p^2) \sim p^{4\kappa-2} = p^{2a_D-2}$ [implying $D(0) = 0$ if $\kappa > 0.5$] for the gluon propagator and of the form $G(p^2) \sim p^{-2\kappa-2} = p^{-2a_G-2}$ for the ghost propagator, with the same exponent κ (i.e. with $a_D = 2a_G$). (These results have been recently criticized in Ref. [22].) The available predictions for the IR exponent point to-

wards $\kappa \gtrsim 0.5$ for pure $SU(N_c)$ gauge theory in the four dimensional case. For the $3d$ case the exponents are $a_G \approx 0.4$ and $a_D \approx 1.3$. Note that in the d dimensional case [19, 20] the relation between a_D and a_G is given by $a_D = 2a_G + (4-d)/2$, implying for the quantity $\alpha(p^2) = (g^2/4\pi)D(p^2)G^2(p^2)p^6$ the infrared behavior $p^{2(a_D-2a_G)} = p^{4-d}$.

Numerical studies of lattice gauge theories confirm the IR divergence of the Landau ghost propagator [23, 24, 25, 26] and have now also established that the Landau gluon propagator shows a turnover in the IR region, attaining a finite value for $p \approx 0$. (A reliable extrapolation of $D(0)$ to the infinite-volume limit is still lacking [18].) More precisely, indications of a decreasing gluon propagator for small p have been obtained in the $4d$ $SU(2)$ and $SU(3)$ cases for the strong-coupling regime [15, 24, 27], in the $3d$ $SU(2)$ case (also in the scaling region) [16, 28, 29], in the $3d$ $SU(2)$ adjoint Higgs model [29] and in the $4d$ $SU(2)$ case at finite temperature [30]. The actual turning of the gluon propagator has been seen clearly for the equal-time three-dimensional transverse gluon propagator in $4d$ $SU(2)$ Coulomb gauge [31, 32], for the $3d$ $SU(2)$ Landau case using very large lattices [18] (of 140 lattice sites per direction) and — recently — in the $4d$ $SU(3)$ Landau case with the use of asymmetric lattices [33, 34, 35, 36].

In this work we extend the study presented in [18] for the $3d$ $SU(2)$ case, by including results for the ghost propagators from very large lattices and by considering also asymmetric lattices, as done in [33, 34, 35, 36, 37]. Our aim is to verify possible systematic effects related to the use of asymmetric lattices, by comparing the results to the ones obtained for symmetric lattices. In particular, we focus on the determination of the IR critical exponents a_D and a_G and on their extrapolation to the infinite-volume limit. The study of gluon and ghost propagators in three space-time dimensions is computationally much simpler than in the four-dimensional case and it may help to get a better understanding of the $4d$ case [38, 39]. Note that the $3d$ case is also of interest in finite-temperature QCD (see for example [40, 41]).

In the following we describe our simulations (see Sec-

tion II) and present our numerical results (see Section III). We end with our conclusions.

II. SIMULATIONS

Simulations have been done using the standard Wilson action for $SU(2)$ lattice gauge theory in three dimensions with periodic boundary conditions. We consider $\beta = 3.4$ and several lattice volumes, up to $V = 140^3$. In Table I we report, for each lattice volume V , the parameters used for the simulations. All our runs start with a random gauge configuration. We used the *hybrid overrelaxed* algorithm (HOR) [42, 43] for thermalization and the *stochastic overrelaxation* algorithm or the so-called *Cornell method* for gauge-fixing thermalized configurations to the lattice Landau gauge [44, 45, 46]. The numerical code is parallelized using MPI [47]. For the random number generator we use a double-precision implementation of RANLUX (version 2.1) with luxury level set to 2. Computations were performed on the PC clusters at the IFSC-USP. We ran part of the 60^3 lattices on three nodes and the 140^3 lattices on four or eight nodes.

In order to set the physical scale we consider $3d SU(2)$ lattice results for the string tension and the input value $\sqrt{\sigma} = 0.44 \text{ GeV}$, which is a typical value for this quantity in the $4d SU(3)$ case. With $\hbar = c = 1$, this implies $1 \text{ fm}^{-1} = 0.4485\sqrt{\sigma}$. For $\beta = 3.4$ we obtain the average plaquette value $\langle W_{1,1} \rangle = 0.672730(3)$. Then, considering the tadpole-improved coupling $\beta_I \equiv \beta \langle W_{1,1} \rangle$, we can evaluate the string tension $\sqrt{\sigma}$ in lattice units using the fit¹ reported in Eq. 2 and Table IV of Ref. [48]. This gives $\sqrt{\sigma} = 0.506(5)$, implying a lattice spacing $a = 0.227(2) \text{ fm}$, i.e. $a^{-1} = 0.869(8) \text{ GeV}$. Also, with the lattice vol-

TABLE I: The lattice volumes V considered for the simulations, the number of configurations, the numbers of HOR sweeps used for thermalization and between two consecutive configurations (used for evaluating the gluon and the ghost propagators).

V	Configurations	Thermalization	Sweeps
20^3	500	550	50
$20^2 \times 40$	800	440	40
$20^2 \times 60$	600	550	50
60^3	400	1100	100
$8^2 \times 64$	100	550	50
$8^2 \times 140$	1000	550	50
$12^2 \times 140$	600	660	60
$16^2 \times 140$	600	770	70
140^3	101	1650	150

¹ The fit is valid for $\beta \gtrsim 3.0$, i.e. the coupling β considered here is well above the strong-coupling region.

umes and the β value used here we are able to consider momenta as small as $p_{min} = 39.0(4) \text{ MeV}$ and physical lattice sides almost as large as 32 fm . Finally, let us notice that, if we compare the data for the string tension (in lattice units) with the the data reported in Ref. [49] for the $SU(2)$ group in four dimensions (see also Ref. [26]), then our value of β corresponds to $\beta \approx 2.21$ in the four dimensional case.

In this work we did not do a systematic study of Gribov-copy effects [24, 50, 51, 52, 53, 54, 55, 56, 57] for the two propagators, since here we are interested in possible systematic effects due to the use of asymmetric lattices. Let us recall that evidences of Gribov-copy effects in lattice Landau gauge have been found by various authors [24, 54, 55, 56, 57] for the ghost propagator and, recently, also for the gluon propagator [53, 57], these effects being usually stronger at small momenta. Such effects have also been found [50, 54] for the horizon tensor (and for the horizon function), for the smallest eigenvalue of the Faddeev-Popov matrix, for the Kugo-Ojima parameter and for the running coupling constant (defined using gluon and ghost propagators).

Here, we also do not check for possible effects from the breaking of rotational invariance [58, 59]. Nevertheless, as we will see below, systematic effects due to the use of asymmetric lattices are evident mostly in the IR limit, where one expects the breaking of the rotational symmetry to play a small effect (see also Ref. [18]).

III. RESULTS

We study the lattice gluon and ghost propagators [respectively, $D(p^2)$ and $G(p^2)$] as a function of the magnitude of the lattice momentum $p(k)$ (see Ref. [16, 60] for definitions). In our simulations we consider all vectors $k \equiv (k_x, k_y, k_t)$ with only one component different from zero and average over the three directions (for the symmetric lattices only). Errors represent one standard deviation.

In Figures 1, 2 and 3 we plot the data obtained for the gluon propagator for different lattice volumes. One can clearly see that the propagator is IR-suppressed for sufficiently large lattice volumes. This behavior is evident both for the asymmetric and the symmetric lattices. However, the shape of the propagator is clearly different in the two cases for momenta $p \lesssim 0.75/a$, i.e. $p \lesssim 0.65 \text{ GeV}$. Indeed, for asymmetric lattices the gluon propagator starts to decrease only at very small momenta (see Figures 1 and 2). A similar behavior can also be observed in Fig. 2 of Ref. [34] and in Fig. 4 of Ref. [36]. Thus, considering the asymmetric lattices one would estimate a value $M \lesssim 0.25/a \approx 0.22 \text{ GeV}$ as a turnover point in the IR, i.e. the momentum $p = M$ for which the propagator reaches its peak. On the other hand, considering the two largest lattice volumes, i.e. $V = 60^3$ (see Fig. 1) and $V = 140^3$ (see Fig. 2), the gluon propagator is clearly a decreasing function of p for $p \lesssim 0.5/a$,

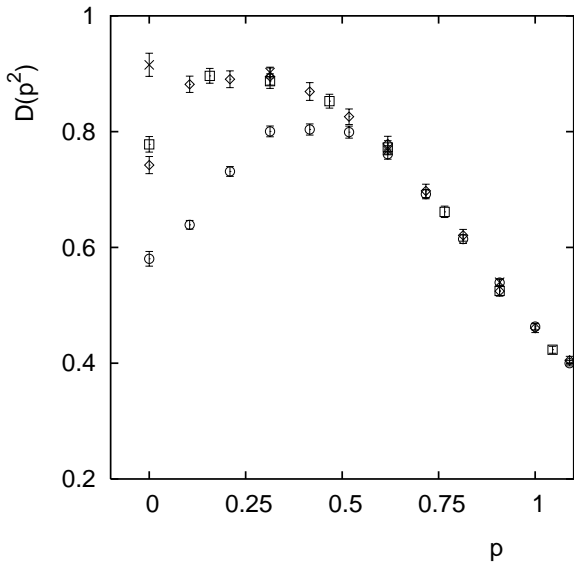


FIG. 1: Plot of the gluon propagator $D(p^2)$ as a function of p (both quantities are given in lattice units) for $\beta = 3.4$ and lattice volumes $V = 20^3$ (\times), $20^2 \times 40$ (\square), $20^2 \times 60$ (\diamond) and $V = 60^3$ (\circ).

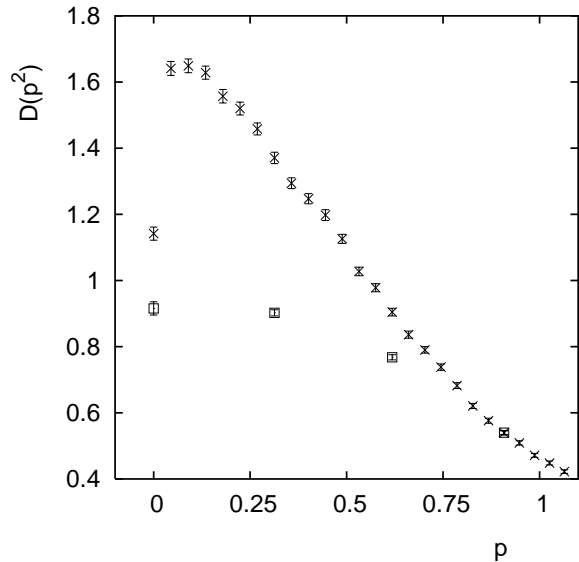


FIG. 3: Plot of the gluon propagator $D(p^2)$ as a function of p (both quantities are given in lattice units) for $\beta = 3.4$ and lattice volumes $V = 8^2 \times 140$ (\times) and 20^3 (\square).

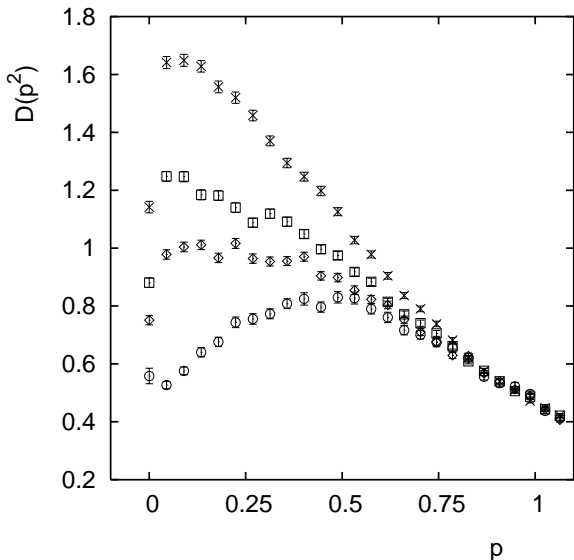


FIG. 2: Plot of the gluon propagator $D(p^2)$ as a function of p (both quantities are given in lattice units) for $\beta = 3.4$ and lattice volumes $V = 8^2 \times 140$ (\times), $12^2 \times 140$ (\square), $16^2 \times 140$ (\diamond) and $V = 140^3$ (\circ).

corresponding to $M \lesssim 0.435$ GeV. This is in agreement with Refs. [16, 18] where the value $M = 350_{-50}^{+100}$ MeV is reported. We thus see a difference of almost a factor 2 between the values obtained for the momentum turnover point in the symmetric and asymmetric cases.

Let us also note that in Figures 1 and 2 the gluon propagator at zero momentum $D(0)$ is monotonically decreasing

TABLE II: Fit of the gluon dressing function $Z(p^2) = D(p^2)p^2$ using the fitting function $z(p^2)^{a_D}(1 + a_1 p^2 + a_2 p^4)$ and data in the interval $p^2 \leq 0.85/a^2$. For each lattice volume V we report the value of the infrared exponent a_D , the number of degrees of freedom (*d.o.f.*) and the $\chi^2/d.o.f.$ For the lattice volume $V = 20^2$ there were not enough data points to do the fit.

V	a_D	$\chi^2/d.o.f.$	#d.o.f.
$20^2 \times 40$	1.026 (7)	0.4	2
$20^2 \times 60$	1.028 (5)	0.4	5
60^3	1.133 (9)	1.1	5
$8^2 \times 64$	0.94 (4)	1.2	5
$8^2 \times 140$	0.981 (5)	1.3	17
$12^2 \times 140$	0.991 (5)	1.2	17
$16^2 \times 140$	1.019 (6)	1.2	17
140^3	1.13 (1)	1.2	17

when considered as a function of the lattice volume V . On the other hand, if one considers the symmetric lattice $V = 20^3 = 8000$ and the slightly larger asymmetric lattice $V = 8^2 \times 140 = 8960$, one finds (see Figure 3) that $D(0)$ is larger (by about 20%) in the asymmetric case. Thus, an extrapolation of $D(0)$ to infinite volume using data from asymmetric lattices is most likely also affected by systematic effects.

We also tried a fit to the data using the fitting functions considered in Ref. [36] (see results in Table II). We see that the IR exponent a_D usually increases with the lattice volume, in agreement with the results reported in Table 2 of Ref. [36]. However, it is clear from Figure 4 that the dependence of a_D on $1/V$ is not simple. Indeed, a_D

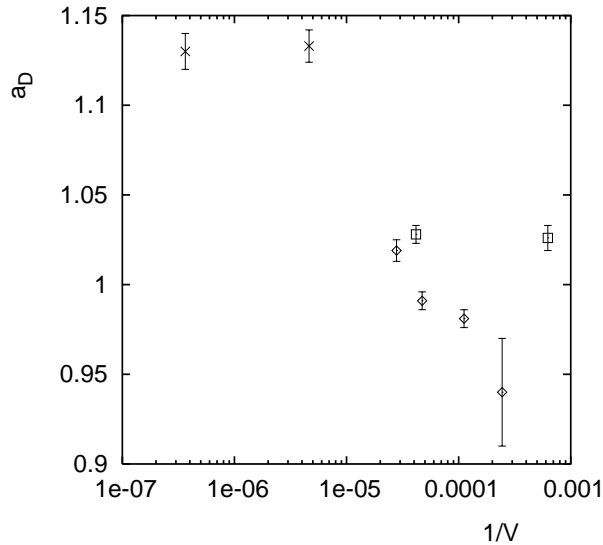


FIG. 4: Plot of the gluon IR exponent a_D as a function of the inverse lattice volume $1/V$ (in lattice units) for $\beta = 3.4$ and lattice volumes: $V = 20^2 \times 40$ and $20^2 \times 60$ (\square), $V = 8^2 \times 64$, $8^2 \times 140$, $12^2 \times 140$ and $16^2 \times 140$ (\diamond), $V = 60^3$ and 140^3 (\times). Note the logarithmic scale on the x axis.

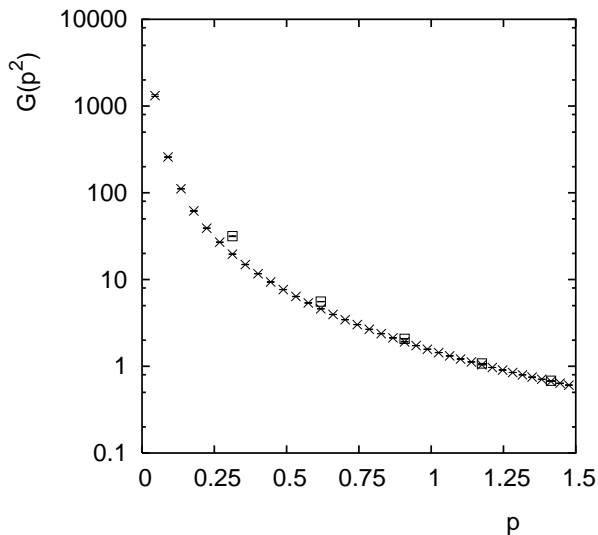


FIG. 5: Plot of the ghost propagator $G(p^2)$ as a function of p (both quantities are given in lattice units) for $\beta = 3.4$ and lattice volumes $V = 8^2 \times 140$ (\times) and 20^3 (\square). Note the logarithmic scale on the y axis.

looks almost constant when considering $V = 20^2 \times 40$ and $20^2 \times 60$, but it gets a larger value when using the symmetric — and much larger — lattice volumes $V = 60^3$ and 140^3 . A smaller value for a_D is also found if one tries an extrapolation as a function of $1/V$ for the results obtained using the three asymmetric lattices $V =$

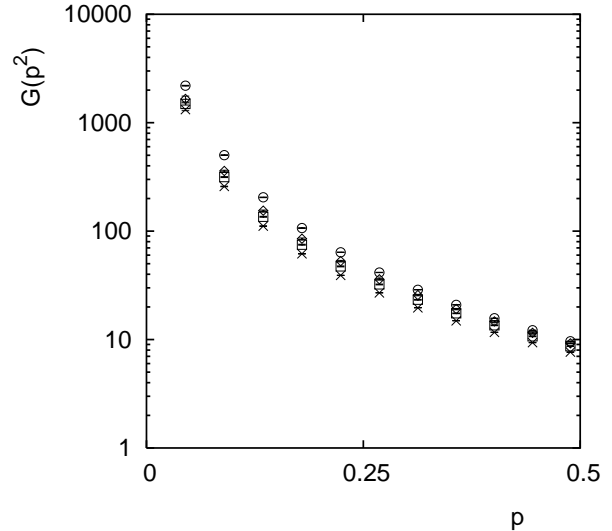


FIG. 6: Plot of the ghost propagator $G(p^2)$ as a function of p (both quantities are given in lattice units) for $\beta = 3.4$ and lattice volumes $V = 8^2 \times 140$ (\times), $12^2 \times 140$ (\square), $16^2 \times 140$ (\diamond) and $V = 140^3$ (\circ). Note the logarithmic scale on the y axis.

TABLE III: Fit of the ghost propagator $G(p^2)$ using the fitting function $z/((p^2)^{1+a_G}(1+a_1p^2+a_2p^4))$ and data in the interval $p^2 \leq 2/a^2$. For each lattice volume V we report the value of the infrared exponent a_G , the number of degrees of freedom (*d.o.f.*) and the value of $\chi^2/d.o.f.$

V	a_G	$\chi^2/d.o.f.$	# <i>d.o.f.</i>
20^3	0.272 (6)	0.4	1
$20^2 \times 40$	0.18 (1)	4.9	6
$20^2 \times 60$	0.154 (9)	3.9	11
60^3	0.21 (1)	4.6	11
$8^2 \times 64$	0.053 (7)	1.7	12
$8^2 \times 140$	0.025 (2)	1.9	31
$12^2 \times 140$	0.060 (4)	2.0	31
$16^2 \times 140$	0.093 (6)	2.0	31
140^3	0.174 (7)	8.5	31

$8^2 \times 140$. Again, it could be difficult to have systematic errors under control when trying an extrapolation using only asymmetric lattices.

Strong systematic effects can also be observed in the ghost case. The propagator is less divergent (at small momenta) when one considers asymmetric lattices (see Figures 5 and 6). As a consequence, the IR exponent a_G is also smaller (see Table III) for asymmetric lattices. This is the case either when comparing an asymmetric lattice to a symmetric one with almost equal lattice volume (i.e. $V = 8^2 \times 140$ and $V = 20^3$) or when considering an asymmetric lattice and a symmetric one with the same largest lattice side (e.g. $V = 16^2 \times 140$ and $V = 140^3$). Moreover, the dependence on the lattice volume is very

different in the two cases. Indeed, for symmetric lattices (e.g. $V = 20^3$, 60^3 and 140^3), the IR exponent decreases as the lattice volume V increases (at fixed β). This is in agreement with the result obtained in the $4d$ $SU(2)$ case (see Table 4 and Figure 3 in Ref. [24]). On the other hand, a_G increases as a function of V for the lattices $V = N_s^2 \times 140$ with increasing N_s . Thus, there is no simple relation between a_G and V and an extrapolation in V using asymmetric lattices is probably of difficult interpretation.

Using the above results we can evaluate the quantity $a_D - 2a_G - 1/2$, which is zero using DSE's [19, 20]. We find $a_D - 2a_G - 1/2 = 0.21(2)$ for $V = 60^3$ and $0.28(2)$ for $V = 140^3$. For the asymmetric lattices this value is somewhat larger. However, let us note that these results depend on the choice of the fitting function. Moreover, the null value for $a_D - 2a_G - 1/2$ should be obtained only in the infinite-volume and in the continuum limit. We will analyze these limits in a future study.

IV. CONCLUSIONS

We have compared data for gluon and ghost propagators (in minimal Landau gauge) obtained using symmetric and asymmetric lattices. We find, for both propagators, clear evidences of systematic effects at relatively small momenta ($p \lesssim 650\text{MeV} \approx 1.5\sqrt{\sigma}$). In particular, the gluon (respectively, ghost) propagator is less suppressed (respec. enhanced) in the IR limit when consid-

ering asymmetric lattices than for the case of symmetric lattices. This implies that the estimates for the IR critical exponents a_G and a_D are systematically smaller in the asymmetric case compared to the symmetric one. Also, for the gluon propagator, the turnover point M is significantly smaller when considering asymmetric lattices than for the symmetric ones. Let us recall that M corresponds to the Gribov mass scale in a Gribov-like propagator $D(p^2) = p^2/(p^4 + M^4)$. Finally, we have seen that the extrapolation to infinite volume of results obtained using asymmetric lattices is also most likely affected by systematic errors.

Our data have been obtained in the $3d$ $SU(2)$ case. However, the behavior observed for the gluon propagator is very similar to what is obtained in the $4d$ $SU(3)$ case [33, 34, 35, 36], where of course a study of this type is more complicated.

Thus, even though using an asymmetric lattice does not modify the qualitative behavior of the two propagators, one should be careful in extracting quantitative information from such studies.

ACKNOWLEDGMENTS

The authors thank A. Maas for helpful comments and suggestions. Research supported by FAPESP (Projects No. 00/05047-5). Partial support from CNPq is also acknowledged.

-
- [1] R. Alkofer and L. von Smekal, Phys. Rept. **353**, 281 (2001).
 - [2] A. Hoell, C. D. Roberts and S. V. Wright, `nucl-th/0601071`.
 - [3] V. N. Gribov, Nucl. Phys. B **139**, 1 (1978);
 - [4] D. Zwanziger, Nucl. Phys. B **412**, 657 (1994).
 - [5] R. F. Sobreiro, S. P. Sorella, D. Dudal and H. Verschelde, Phys. Lett. B **590**, 265 (2004).
 - [6] D. Dudal, R. F. Sobreiro, S. P. Sorella and H. Verschelde, Phys. Rev. D **72**, 014016 (2005).
 - [7] R. F. Sobreiro and S. P. Sorella, `hep-th/0504095`, lectures given at *13th Jorge Andre Swieca Summer School on Particle and Fields*, Campos do Jordão, Brazil, 2005.
 - [8] T. Kugo and I. Ojima, Prog. Theor. Phys. Suppl. **66**, 1 (1979); Erratum – Prog. Theor. Phys. **71**, 1121 (1984).
 - [9] T. Kugo, `hep-th/9511033`, in the Proceedings of the *International Symposium on BRS Symmetry on the Occasion of its 20th Anniversary*, Kyoto, Japan, 1995, edited by M. Abe, N. Nakanishi and I. Ojima, (Universal Academy Press, Tokyo, 1996, FSS 17).
 - [10] D. Zwanziger, Phys. Lett. B **257**, 168 (1991).
 - [11] D. Zwanziger, Nucl. Phys. B **364**, 127 (1991).
 - [12] D. Zwanziger, Nucl. Phys. B **378**, 525 (1992).
 - [13] A. Cucchieri, T. Mendes and A. R. Taurines, Phys. Rev. D **71**, 051902(R) (2005).
 - [14] S. Furui and H. Nakajima, Phys. Rev. D **70**, 094504 (2004).
 - [15] A. Cucchieri, Phys. Lett. B **422**, 233 (1998).
 - [16] A. Cucchieri, Phys. Rev. D **60**, 034508 (1999).
 - [17] F. D. Bonnet et al., Phys. Rev. D **64**, 034501 (2001).
 - [18] A. Cucchieri, T. Mendes and A. R. Taurines, Phys. Rev. D **67**, 091502(R) (2003).
 - [19] D. Zwanziger, Phys. Rev. D **65**, 094039 (2002).
 - [20] C. Lerche and L. von Smekal, Phys. Rev. D **65** (2002) 125006.
 - [21] R. Alkofer, W. Detmold, C. S. Fischer and P. Maris, Phys. Rev. D **70**, 014014 (2004).
 - [22] P. Boucaud *et al.*, `hep-ph/0507104`.
 - [23] H. Suman and K. Schilling, Phys. Lett. B **373**, 314 (1996).
 - [24] A. Cucchieri, Nucl. Phys. B **508**, 353 (1997).
 - [25] S. Furui and H. Nakajima, Phys. Rev. D **69**, 074505 (2004).
 - [26] J. C. R. Bloch, A. Cucchieri, K. Langfeld and T. Mendes, Nucl. Phys. B **687**, 76 (2004).
 - [27] H. Nakajima and S. Furui, Nucl. Phys. Proc. Suppl. **73**, 635 (1999).
 - [28] A. Cucchieri, F. Karsch and P. Petreczky, Phys. Lett. B **497**, 80 (2001).
 - [29] A. Cucchieri, F. Karsch and P. Petreczky, Phys. Rev. D **64**, 036001 (2001).
 - [30] I. L. Bogolubsky and V. K. Mitrjushkin, `hep-lat/0204006`.
 - [31] A. Cucchieri and D. Zwanziger, Phys. Rev. D **65**, 014001

- (2002).
- [32] A. Cucchieri and D. Zwanziger, Phys. Lett. B **524**, 123 (2002).
- [33] O. Oliveira and P. J. Silva, AIP Conf. Proc. **756**, 290 (2005).
- [34] P. J. Silva and O. Oliveira, PoS **LAT2005**, 286 (2005).
- [35] O. Oliveira and P. J. Silva, PoS **LAT2005**, 287 (2005).
- [36] P. J. Silva and O. Oliveira, hep-lat/0511043.
- [37] M. B. Parappilly et al., hep-lat/0601010.
- [38] R. P. Feynman, Nucl. Phys. B **188**, 479 (1981).
- [39] J. M. Cornwall, PhysicaA **158**, 97 (1989).
- [40] F. Karsch, M. Oevers and P. Petreczky, Phys. Lett. B **442**, 291 (1998).
- [41] A. Maas, Mod. Phys. Lett. A **20**, 1797 (2005).
- [42] F. R. Brown and T. J. Woch, Phys. Rev. Lett. **58**, 2394 (1987).
- [43] U. Wolff, Phys. Lett. B **288**, 166 (1992).
- [44] A. Cucchieri and T. Mendes, Nucl. Phys. B **471**, 263 (1996).
- [45] A. Cucchieri and T. Mendes, Nucl. Phys. Proc. Suppl. **53**, 811 (1997).
- [46] A. Cucchieri and T. Mendes, Comput. Phys. Commun. **154**, 1 (2003).
- [47] A. Cucchieri, T. Mendes, G. Travieso and A. R. Taurines, hep-lat/0308005, in the Proceedings of the *15th Symposium on Computer Architecture and High Performance Computing*, São Paulo SP, Brazil, 2003, edited by L.M. Sato et al., (IEEE Computer Society Press, Los Alamitos CA, 2003) 123–131.
- [48] B. Lucini and M. Teper, Phys. Rev. D **66**, 097502 (2002).
- [49] J. Fingberg, U. M. Heller and F. Karsch, Nucl. Phys. B **392**, 493 (1993).
- [50] A. Cucchieri, Nucl. Phys. B **521**, 365 (1998).
- [51] L. Giusti et al., Int. J. Mod. Phys. A **16**, 3487 (2001).
- [52] J. E. Mandula, Phys. Rept. **315**, 273 (1999).
- [53] P. J. Silva and O. Oliveira, Nucl. Phys. B **690**, 177 (2004).
- [54] H. Nakajima and S. Furui, Nucl. Phys. Proc. Suppl. **141**, 34 (2005).
- [55] A. Sternbeck, E. M. Ilgenfritz, M. Muller-Preussker and A. Schiller, Nucl. Phys. Proc. Suppl. **140**, 653 (2005).
- [56] A. Y. Lokhov, O. Pene and C. Roiesnel, hep-lat/0511049.
- [57] I. L. Bogolubsky, G. Burgio, M. Muller-Preussker and V. K. Mitrjushkin, hep-lat/0511056.
- [58] D. Becirevic et al., Phys. Rev. D **60**, 094509 (1999).
- [59] J. P. Ma, Mod. Phys. Lett. A **15**, 229 (2000).
- [60] A. Cucchieri, T. Mendes and A. Mihara, Phys. Rev. D **72**, 094505 (2005).